Size dependence of "effective" barrier heights of mixed-phase contacts

J. L. Freeouf, T. N. Jackson, S. E. Laux, and J. M. Woodall

IBM Research, P.O.Box 218, Yorktown Heights, New York 10598

(Received 26 January 1982; accepted 22 March 1982)

The literature currently abounds with experimental studies of Schottky barrier heights of various metals upon many semiconductors. Unfortunately, these studies present some puzzling aspects: (1) Commonly, barriers determined by C–V studies are larger than barriers determined by I–V studies, and (2) Results obtained by different workers under apparently identical conditions are not always similar. A possible explanation for such effects is simply that many/most contacts experimentally achieved are in fact multiphase; these different barrier-height regions could result from variations in the metallurgical reactions assumed by many current models of Schottky barrier energetics. The different barrier heights measured by different techniques follow directly from the functional form of the relevant probes (e.g., I–V would more heavily weight a low-barrier region). The lack of reproducibility would follow from kinetic aspects of the relevant metallurgical interactions. A recent publication discusses the functional form for I–V and C–V "effective" barrier heights from mixed-phase contacts *isolated* from one another. These results apply directly to mixed-phase contacts **only** if the linear dimensions of all contact regions are large compared to the Debye length of the substrate ($\approx 0.1\,\mu$ for 10^{15} silicon). In this paper, we examine the effects of contact dimensions upon equilibrium potentials (e.g., band bending) as well as transport studies to infer "effective" barrier heights for truly mixed-phase contacts of varying dimensions but **fixed** area ratios.

PACS numbers: 73.30. + y

The literature currently abounds with experimental studies of Schottky barrier heights of various metals upon many semiconductors. However, barriers determined by C–V studies are often larger than barriers determined by I–V studies.[1] Furthermore, barriers deduced *via* identical techniques for apparently comparable preparation procedures often vary greatly.[2] A possible explanation for such effects is simply that many/most contacts experimentally achieved are in fact multiphase; these different barrier-height regions could result from variations in the metallurgical reactions assumed by many current models of Schottky barrier energetics.[3–6] The different barrier heights measured by different techniques follow directly from the functional form of the relevant probes (e.g., I–V would heavily weight a low-barrier region).[7] A lack of reproducibility would follow from kinetic aspects of the relevant metallurgical interactions.

A recent publication[7] discusses the functional form for I–V and C–V effective barrier heights from mixed-phase contacts *isolated* from one another. The authors demonstrated that barrier height and area ratio of the two phases totally determined the effective barrier heights. These results apply directly to mixed-phase contacts **only** if the linear dimensions of all contact regions are large compared to the Debye length of the substrate (i.e., $\gg 0.1\mu$ for 10^{15} carriers/cm^3 n-silicon). The reason for this limitation is that the analysis of Ref. 7 neglected the constraints of continuous fields within the semiconductor; as was noted[7] in the reference, this assumption is only valid for large contacts. For small regions, however, this requirement can vastly alter the space–charge region under the contacts—and therefore alter the observed transport and band bending. In this paper, we examine the effects of contact dimensions upon transport studies to infer effective barrier heights for truly mixed-phase contacts of varying dimensions but **fixed** area ratios.

Mixed-phase contact structures were simulated using FIELDAY, a finite element device analysis program[8,9] that simultaneously solves Poisson's equation and the current continuity equations in two dimensions; the calculations were performed both at equilibrium and away from equilibrium, thereby permitting direct simulation of the common experimental probes used to determine Schottky barrier heights. I–V data are determined directly from this device simulation program; C–V data are calculated using a new technique[10] based on the two–dimensional space–charge distribution.

In Figs. 1 and 2 we demonstrate the effects under discussion. In these figures we plot potential contours under equi-

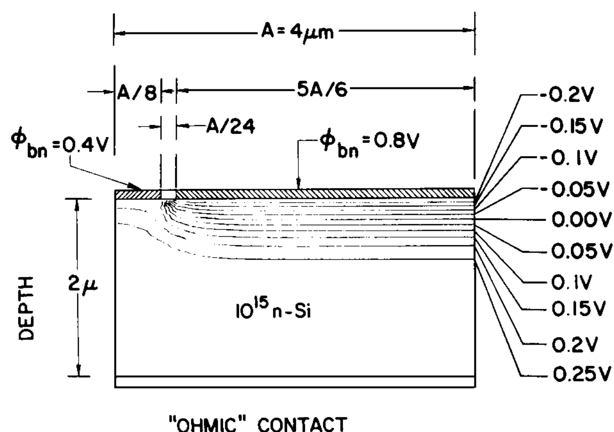

FIG. 1. Contour plot of equilibrium potential distribution for 4μ contact discussed in Table I. Geometries used in these calculations are also illustrated.

 0022-5355/82/060570-04$01.00 © 1982 American Vacuum Society

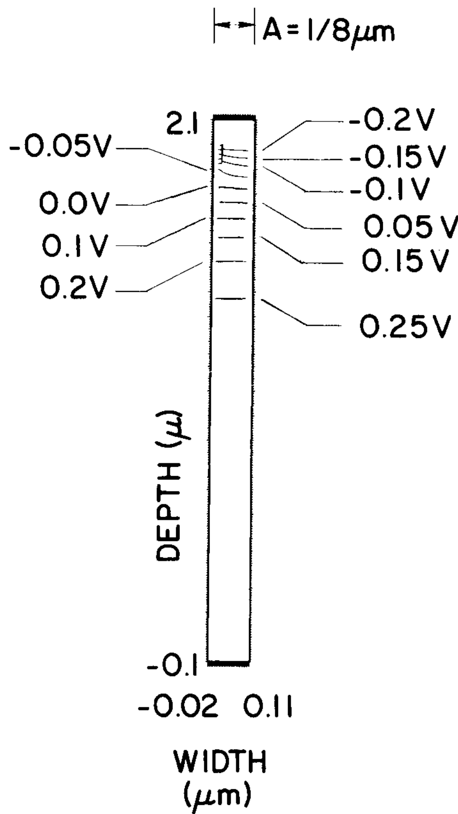

FIG. 2. Contour plot of equilibrium potential distribution for the $1/8\mu$ contact discussed in Table I.

librium conditions (zero bias) for two mixed-phase contacts identical in all respects except for their spatial extent. The geometry used is illustrated in Fig. 1; a 0.4 V contact with $\approx 1/8$ the total area is imbedded in a large barrier (0.8 V) region of area 5/6 the total (there is a gap of 1/24 the total area). The program is told that the substrate has silicon para-

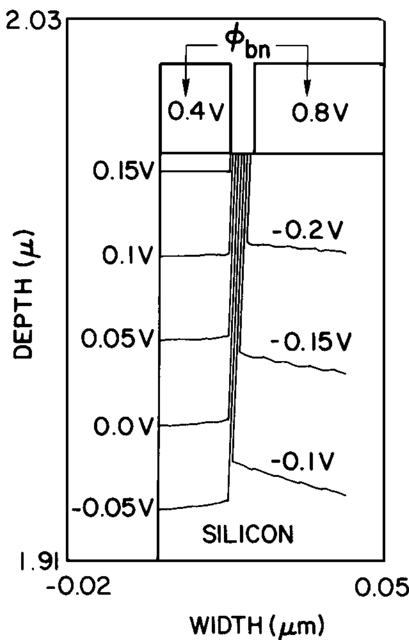

FIG. 3. Expanded scale plot of a portion of Fig. 2.

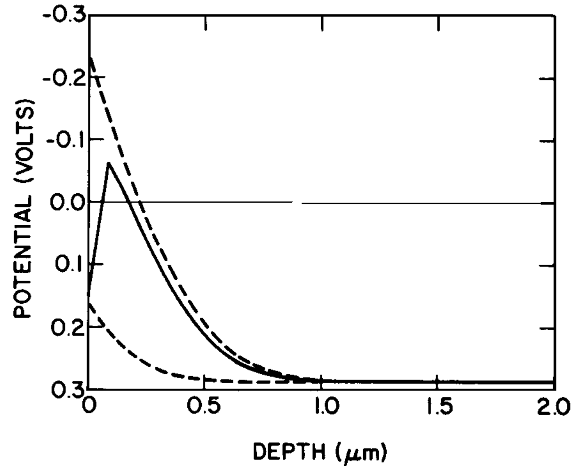

FIG. 4. One-dimensional plot of equilibrium potential distribution for three cases. The dotted lines are the results for single-phase contacts of $\phi_{bn} = 0.8$ and 0.4 V (the upper curve is the 0.8 V barrier). The solid curve is the result for the **center** of a 0.4 V contact of total width $1/32\mu$ (the 1/8 contact of Table I).

meters (n-type, $10^{15}/cm^3$) and is 2μ thick. The bottom side is contacted by an "ohmic" contact defined by charge neutrality. Mirror-symmetry boundary conditions are specified at the edges of the contact; thus, the "true" width of the low- and high-barrier regions is effectively twice that shown. The total contact width is therefore 8μ for Fig. 1, and $1/4\mu$ for Fig. 2; the 0.4 V contact is 1μ wide in Fig. 1 and $1/32\mu$ wide in Fig. 2. These symmetry assumptions constrain the potential contours to be flat at the symmetry planes, as can be seen at the edges of these figures; these edges are effectively the **centers** of the low- and high-barrier contacts. The program further assumes zero spatial variation in the third dimension (i.e., length is assumed infinite). All potentials in this paper are referenced to E_i, the intrinsic Fermi level at the midgap of silicon; the sign is such that a negative potential places E_F **below** E_i, and therefore implies a large barrier to n-Si. The effects of the change in spatial extent are clearly demonstrated by the occurrence of potentials 0.2 V **more negative** in the region under the low-barrier contact in Fig. 2 than occurs in

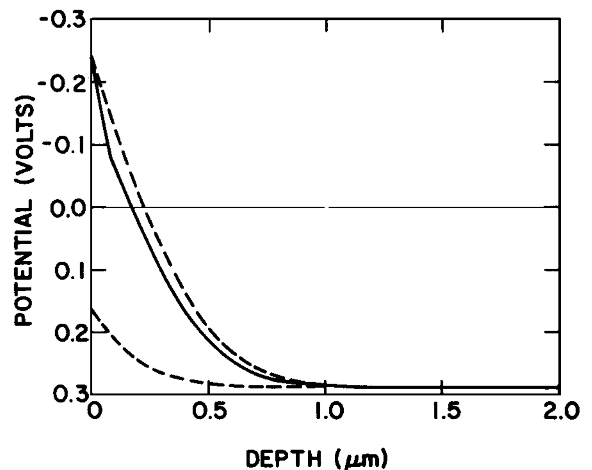

FIG. 5. Same as Fig. 4, except the solid line is the potential at the **edge** of the 0.8 V contact closest to the lower barrier region.

TABLE I. Barrier heights extracted by standard techniques from computer-simulated current and charge response to bias variations. The contacts denoted by sizes contain a 0.8 V barrier of 5/6 the total area, and a 0.4 V contact of 1/8 the total area. The width of the 0.4 V contact is 1/4 times the size shown in the second column ("A" in Fig. 1). The *I–V* results are two-point fits using forward bias of 0.05 and 0.1 V (0.1 and 0.2 V).

Material		*C–V*		*I–V*	
Symbol	Size	Barrier (V)	Doping (cm^{-3})	Barrier (V)	Ideality
+	4 μ	0.681	9.41×10^{14}	0.461 (0.431)	1.57 (2.92)
x	2 μ	0.716	9.73×10^{14}	0.48 (0.45)	1.42 (2.39)
□	1 μ	0.734	9.91×10^{14}	0.529 (0.509)	1.25 (1.68)
○	0.5 μ	0.741	9.99×10^{14}	0.59 (0.577)	1.15 (1.34)
△	0.25 μ	0.742	1.00×10^{15}	0.635 (0.625)	1.09 (1.22)
*	0.125 μ	0.742	1.001×10^{15}	0.66 (0.65)	1.06 (1.17)
Single phase					
0.8 Barrier		0.800	1.00×10^{15}	0.800 (0.793)	0.94 (1.00)
0.4 Barrier		0.401	1.01×10^{15}	0.401 (0.374)	1.8 (3.54)

the comparable region in Fig. 1. The region of most interest in Fig. 2 is shown on an expanded scale in Fig. 3, permitting a more detailed study of the matching of potentials between the two contacts in this mixed-phase contact of overall dimensions ≈ Debye length. In Fig. 4 we present a one-dimensional plot of the potentials versus depth of a "pure" (single phase) 0.8 V contact, a "pure" 0.4 V contact, and the potential at the center of the 0.4 V contact of the structure of Fig. 2. This plot clearly shows the existence of a barrier underneath the 0.4 V contact that is substantially increased from that of a pure 0.4 V contact. In Fig. 5 we show the same pure potentials, as well as the potential under the 0.8 V contact at the edge **closest** to the 0.4 V contact, again for the structure of Fig. 2; there is a clearly discernible effect, but the absolute barrier height is unaltered.

In Table I we show the effects of varying size upon mixed-phase Schottky barriers of the same fixed area ratio as was used for Figs. 1 and 2. The total contact width simulated is twice that shown in the second column (dimension A of Fig. 1). The table shows the effects of varying the size of this mixed-phase contact upon determinations of "barrier height" by the common techniques of (log I) vs V and by ($1/C^2$) vs V. For comparison, we also show the results obtained by these simulations for the low- and high-barrier contacts by themselves, i.e., as single-phase contacts.

Clearly the absolute size of the two regions strongly affects the barrier height determinations. As the low-barrier height region width gets smaller, it is more effectively "pinched off" by the large barrier contact, leading to a larger "barrier." For comparison, the analytical solution of Ohdomari and Tu[7] (who neglected this effect) gives an *I–V* barrier of 0.449 V, and a *C–V* barrier of 0.662 V. Their result would be the same for all sizes shown, since they did not address size effects.

Figures 6, 7, and 8 show the calculated current and ($1/C^2$) versus applied bias for the various sizes; the symbols denote sizes as shown in Table I. Figure 6 shows the current density versus bias, Fig. 7 shows the logarithm of the current density versus forward bias, and Fig. 8 shows the values of ($1/C^2$) under reverse bias. The points shown in Figs. 7 and 8 were used in the standard procedures of extracting barrier height from experimental data; the capacitance results used all the points, whereas the *I–V* results used only the first two (or the second and third) to avoid resistive effects. Clearly, the ca-

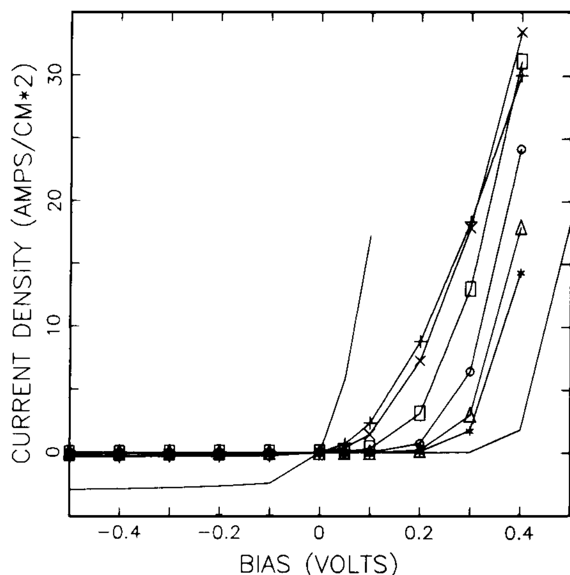

FIG. 6. Current density vs applied voltage for contacts of varying sizes (see text). Symbols denote sizes as indicated in Table I; lines refer to single-phase contacts of 0.8 and 0.2 V barrier height.

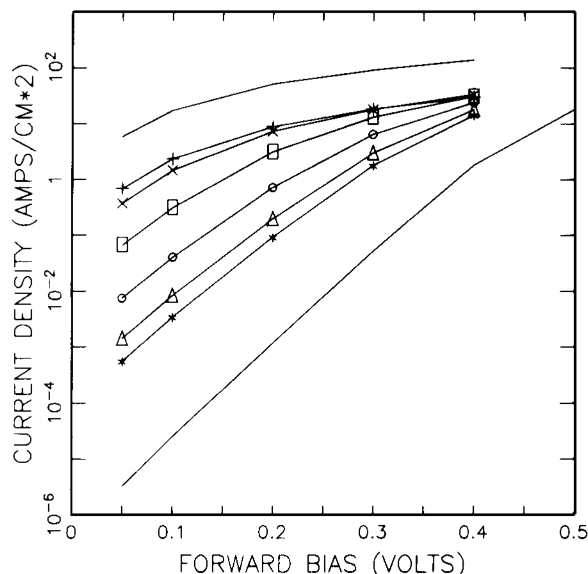

FIG. 7. Logarithm of current density vs forward bias for contacts as discussed in Fig. 6.

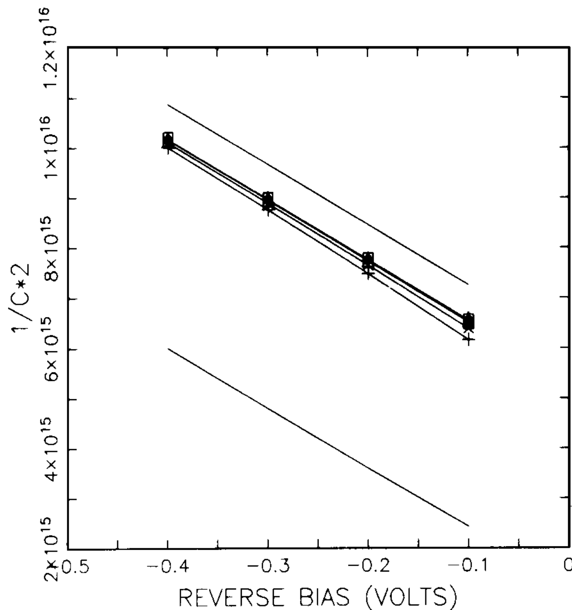

FIG. 8. Square of inverse capacitance vs reverse bias of contacts discussed in Fig. 6 caption (capacitance units are farads/cm^2).

pacitance data alone provides no "warnings" concerning the mixed-phase nature of the contact being studied. The I–V data, especially that from the larger contacts, provides warnings of a resistive effect (apparently the cause of the large idealities sometimes inferred), but many of these contacts would appear to be "normal," single-phase contacts to both techniques. It would appear that transport data from a particular contact would not always give any warning of mixed phases other than a discrepancy between C–V and I–V derived barrier heights. Furthermore, a mixed-phase contact can provide stronger rectification than can the minority phase for low-barrier minority phases. Previously, we demonstrated[11] that a mixed-phase contact can provide strong rectification even if the minority phase is an ohmic contact.[4,12]

A side issue concerning these results can be seen by close examination of Fig. 6. At the larger forward biases, the 4 μ contact permits **less** current density than do the 2 and 1 μ contacts; this result appears contrary to the anticipated trend of smaller dimensions leading to larger barriers. Contour plots of current density (not shown) provide the explanation for this effect, which is derived from spreading resistance arguments. For these contacts at large forward biases, the limiting resistance is provided by the substrate, not the barrier; the smaller overall dimensions of the 2 and 1 μ contact devices permit better utilization of the underlying substrate, whereas current from the 4 μ device cannot adequately spread to the far edge of the device.

It has been suggested that an indicator of mixed-phase contacts is provided by the measurement of barrier heights on both n- and p-type substrates.[13] Since the low-barrier region dominates exponentially (for the independent diode approximations employed), one should obtain log I–V barrier heights to n- and p-substrates that sum to less than the band gap. These seem eminently reasonable arguments; we wondered, however, as to the impact of size effects upon such considerations. To explore this issue, we calculated log I–V barrier heights for a mixed-phase contact to both n- and p-silicon (both doped at $10^{15}/\mathrm{cm}^3$ as in the rest of the paper). We did not calculate C^2–V barriers for this system, since those results should be larger for both n- and p- substrates; the I–V results should provide the largest effect. The barriers used were different, since the 0.8 V contact would be too leaky to p-Si, so we used contacts of $\phi_{\rm bn} = 0.5$ and 0.7 V, with the same area ratios as before, and the 0.7 V $= \phi_{\rm bn}$ as the large-area contact. The overall dimensions were those of the contact of Fig. 2, discussed in Table I as the 1/8 μ contact. The resulting barriers were $\phi_{\rm bn} = 0.617$ V, and $\phi_{\rm bp} = 0.415$ V (using appropriate Richardson's constants for n- and p-Si). These results sum to 1.032; this sum differs from the assumed band gap (1.12) by a quantity possibly discernible by experiment.

These results were all obtained by assuming bulk metal contacts that place the equilibrium interface Fermi level at the same position with respect to the semiconductor valence and conduction bands as would have been achieved by a pure contact. The effects demonstrated in potential distribution and charge transport have all followed from the response of the **bulk** semiconductor to these differing boundary conditions. The assumption that the Fermi-level position **at the interface** is independent of these effects may well be invalid, at least in detail. In particular, for the low coverages often discussed in the surface studies of Schottky barrier formation, one may well expect such interactive effects to occur even at the surface; this means that a surface of "mixed phase" such that two pinning positions should occur may instead, show only one "averaged" surface Fermi-level position.

[1]A. Thanailakis, J. Phys. C **8**, 655 (1975).
[2]T. P. Humphreys, M. H. Patterson, and R. H. Williams, J. Vac. Sci. Technol. **17**, 886 (1980).
[3]J. L. Freeouf, Solid State Commun. **33**, 1059 (1980).
[4]J. L. Freeouf and J. M. Woodall, Appl. Phys. Lett. **39**, 727 (1981).
[5]W. E. Spicer, I. Lindau, P. Skeath, and C. Y. Su, J. Vac. Sci. Technol. **17**, 1019 (1980).
[6]Leonard J. Brillson, J. Vac. Sci. Technol. **16**, 1137 (1979).
[7]I. Ohdomari and K. N. Tu, J. Appl. Phys. **51**, 3735 (1980).
[8]P. E. Cottrell and E. M. Buturla, in *Numerical Analysis of Semiconductor Devices*, edited by B. T. Browne and J. J. H. Miller (Boole, Dublin, 1979), pp. 31–64.
[9]E. M. Buturla, P. E. Cottrell, B. M. Grossman, and K. A. Salsburg, IBM J. Res. Dev. **25**, 218 (1981).
[10]S. E. Laux (to be published).
[11]J. L. Freeouf, T. N. Jackson, S. E. Laux, and J. M. Woodall, Appl. Phys. Lett. **40**, 634 (1982).
[12]C. F. Brucker and L. J. Brillson, Appl. Phys. Lett. **39**, 67 (1981).
[13]K. N. Tu, J. Vac. Sci. Technol. **19**, 766 (1981).